

Kinetics of the Reactions of NO₃ Radical with Methacrylate Esters 2

Li Zhou, A. R. Ravishankara, Steven Brown, Mahmoud Idir, Kyle Zarzana,
Véronique Daële, Abdelwahid Mellouki

► **To cite this version:**

Li Zhou, A. R. Ravishankara, Steven Brown, Mahmoud Idir, Kyle Zarzana, et al.. Kinetics of the Reactions of NO₃ Radical with Methacrylate Esters 2. *Journal of Physical Chemistry A*, American Chemical Society, 2017, 121 (23), pp.4464-4474. 10.1021/acs.jpca.7b02332 . insu-01527239

HAL Id: insu-01527239

<https://hal-insu.archives-ouvertes.fr/insu-01527239>

Submitted on 24 May 2017

HAL is a multi-disciplinary open access archive for the deposit and dissemination of scientific research documents, whether they are published or not. The documents may come from teaching and research institutions in France or abroad, or from public or private research centers.

L'archive ouverte pluridisciplinaire **HAL**, est destinée au dépôt et à la diffusion de documents scientifiques de niveau recherche, publiés ou non, émanant des établissements d'enseignement et de recherche français ou étrangers, des laboratoires publics ou privés.



1
2
3
4
5 **1 Kinetics of the Reactions of NO₃ Radical with Methacrylate**
6
7
8 **2 Esters**
9

10
11 3 Li Zhou,^a A.R. Ravishankara,^{a,b,*} Steven S. Brown,^{c,d} Mahmoud Idir,^a Kyle J. Zarzana,^{c,e}

12
13
14 4 Véronique Daële,^a Abdelwahid Mellouki^{a,*}
15

16
17 5

18
19
20 6 a. Institut de Combustion, Aérothermique, Réactivité et Environnement/OSUC, CNRS, 45071

21
22 7 Orléans Cedex 02, France
23

24
25 8 b. Departments of Chemistry and Atmospheric Science, Colorado State University, Fort Collins,

26
27
28 9 CO 80253, USA
29

30
31 10 c. National Oceanic and Atmospheric Administration, Earth System Research Laboratory,

32
33 11 Chemical Sciences Division, 325 Broadway, Boulder, CO 80305, USA
34

35
36 12 d. Department of Chemistry, University of Colorado, Boulder, CO 80305, USA
37

38
39 13 e. Cooperative Institute for Research in Environmental Sciences, University of Colorado,

40
41
42 14 Boulder, CO 80305, USA
43

44
45 15 *Address correspondence to:

46
47 16 A.R.Ravishankara@colostate.edu or Adelwahid.Mellouki@cnrs-orleans.fr
48
49

50
51 17

52
53 18

54
55
56 19
57
58
59
60

20 Abstract

21 Two different experimental methods (relative rate and absolute rate methods) were
22 used to measure the rate coefficients for the reactions of NO₃ radical with six
23 methacrylate esters: methyl methacrylate (MMA, k₁), ethyl methacrylate (EMA, k₂),
24 propyl methacrylate (PMA, k₃), isopropyl methacrylate (IPMA, k₄), butyl methacrylate
25 (BMA, k₅), isobutyl methacrylate (IBMA, k₆). In the relative rate method, the loss of the
26 esters relative to that of a reference compound was followed in a 7300 L Teflon-walled
27 chamber at (298±2) K and (1000±5) hpa. In the absolute method, the temporal profiles of
28 NO₃ and N₂O₅ were followed using a dual channel cavity ring down spectrometer in the
29 presence of an excess of ester in the 7300 L chamber. The rate coefficients from these two
30 methods (weighted averages) in the units of 10⁻¹⁵ cm³ molecule⁻¹ s⁻¹ at 298 K are: k₁ =
31 (2.98±0.35); k₂ = (4.67±0.49); k₃ = (5.23±0.60); k₄ = (7.9₁±1.0₀); k₅ = (5.71±0.56); and k₆
32 = (6.24±0.66). The quoted uncertainties are at the 2σ level and include estimated
33 systematic errors. Unweighted averages are also reported. In addition, the rate coefficient
34 k₇ for the reaction of NO₃ radical with deuterated methyl methacrylate (MMA-D8) was
35 measured using the relative rate method to be essentially the same as k₁. The trends in the
36 measured rate coefficient with the length and nature of the alkyl group, along with the
37 equivalence of k₁ and k₇ strongly suggests that the reaction of NO₃ with the methacrylate
38 esters proceeds via addition to the double bond on the methacrylate group. The present

1
2
3
4 39 results are compared with those from previous studies. Using the measured values of the
5
6
7 40 rate coefficients, along with those for reactions of these esters with OH, O₃, and chlorine
8
9
10 41 atoms, the atmospheric lifetimes of methacrylate esters are calculated. We suggest that
11
12 42 NO₃ radicals do contribute to the atmospheric loss of these unsaturated esters, but to a
13
14
15 43 lesser extent than their reactions with OH and O₃.
16
17

18 44

19
20 4521
22 4623
24 4725
26 4827
28 4929
30 5031
32 5133
34 5235
36 5337
38 5439
40 5541
42 5643
44 57

1 Introduction

Methacrylate esters are important unsaturated oxygenated volatile organic compounds (OVOCs) used in the production of polymers. They are used extensively for manufacture of industrial products such as resins and plastics. Due to their high volatility, these unsaturated OVOCs may be released into the atmosphere, particularly in industrial areas. For example, more than 5,000 tonnes of methyl methacrylate is produced every year in the European Union. The maximum production capacity in each location methacrylates is estimated to be around 10,000 tonnes per year and release from these facilities are estimated to be between 0.005% to 1.1 % of the production values¹. If emitted, their atmospheric degradation could lead to surface ozone and aerosols formation.

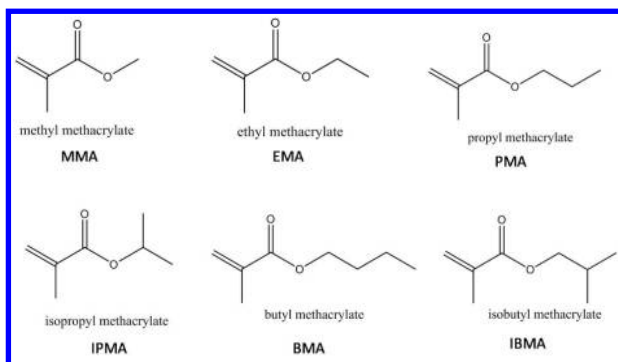
Once released, these unsaturated OVOCs are degraded in the atmosphere by reaction with various reactive species, which include OH and NO₃ radicals, chlorine atoms and O₃.² The nitrate radical, NO₃, is a photochemically unstable radical that is prevalent at night, especially in polluted areas that have large NO_x emissions. NO₃ is known to be an important nighttime oxidant for OVOCs in the atmosphere.³ Therefore, rate coefficients for the reactions of NO₃ radicals with methacrylate esters are needed to assess their atmospheric loss rates, especially at night.

Kinetics and products of reactions of OH radical reactions with acrylates and methacrylates has been the subject of several studies.⁴⁻⁵ Reactions of several methacrylate

1
2
3
4 77 esters with O_3 have also been studied at room temperature.⁶⁻⁷ Rate coefficients for the
5
6
7 78 reactions of chlorine atoms with methyl methacrylate (MMA) and ethyl methacrylate
8
9
10 79 (EMA) have been reported.⁸⁻⁹ Several groups¹⁰⁻¹³ have measured the rate constants for the
11
12 80 reaction of NO_3 with several methacrylates near 298 K via the relative method, often
13
14
15 81 using the reaction of NO_3 with propene as the reference.
16
17

18 82 In this work, we report the room temperature ($298 \pm 2K$) rate coefficients for the
19
20
21 83 reactions of NO_3 radical with six of the methacrylate esters (shown below): methyl
22
23
24 84 methacrylate (MMA) - k_1 ; ethyl methacrylate (EMA) - k_2 ; propyl methacrylate (PMA) - k_3 ;
25
26
27 85 isopropyl methacrylate (IPMA) - k_4 ; butyl methacrylate (BMA) - k_5 ; and isobutyl
28
29
30 86 methacrylate (IBMA) - k_6 .

31
32 87



90 We used two different experimental methods: (1) a relative rate method where the loss
91 of the ester was measured relative to that of a reference compound while competing for a
92 common pool of NO_3 radicals; and (2) a direct method where the temporal profiles of NO_3
93 and N_2O_5 were measured using cavity ring down spectroscopy to detect NO_3 and N_2O_5 in

1
2
3
4 94 an excess of known concentrations of esters. Both N_2O_5 and NO_3 (which are essentially in
5
6
7 95 equilibrium) decay together when NO_3 is lost via its reaction with the hydrocarbon.
8
9
10 96 Therefore, we used a box model consisting of 5 reactions (see later) to simulate the
11
12 97 temporal profiles of NO_3 and N_2O_5 and quantitatively compare them (via least squares
13
14
15 98 method) with the observed profiles of these species. The use of these two complementary
16
17
18 99 methods enhances our confidence in the measured rate coefficients. In addition, the rate
19
20
21 100 coefficient of deuterated methyl methacrylate (MMA-D8) with NO_3 radical was also
22
23
24 101 investigated to shed light on the mechanism of the reaction. Using the obtained kinetics
25
26
27 102 data, the atmospheric lifetimes of methacrylate esters towards NO_3 radicals were
28
29
30 103 calculated and compared with those due to loss via reactions with OH radicals, O_3 and
31
32 104 chlorine atoms (Cl). The kinetics results also enhance the available database on NO_3
33
34
35 105 reactions.
36

37
38 106
39
40
41
42
43
44
45
46
47
48
49
50
51
52
53
54
55
56
57
58
59
60

107 **2 Experiments and Results**

108 In this section, we will describe our results from the two methods that were used.

109 Because the experimental methods were somewhat different, we will first describe the
110 chamber that was used for both methods followed by the analytical methods that were
111 employed. Subsequently, the obtained data are presented.

112 **2.1 Experimental system: Indoor atmospheric simulation chamber**

113 The kinetic of NO_3 with esters were studied at room temperature ($298 \pm 2\text{K}$) in the
114 ICARE-7300L Teflon chamber (Figure1), which has been described in detail.¹⁴⁻¹⁵ We will
115 describe here only the features necessary to understand this study. The chamber was
116 equipped with three key analytical tools: (1) a proton transfer reaction mass spectrometer,
117 which was fed from the center of the chamber, to measure the concentrations of
118 hydrocarbon reactants (and some of the products); (2) a Nicolet 5700 Magna FT-IR
119 spectrometer (which sampled approximately 2m near the center of the chamber) the
120 coupled to a white-type mirror system with roughly 70 passes resulting in an optical path of
121 about 140 m; and (3) a cavity ring down spectrometer fed from the center of the chamber
122 (with its inlet next to that for the PTR-MS) to measure NO_3 and N_2O_5 . (We could also
123 estimate the concentration of NO_2 using this system.) All the three analytical tools sampled
124 essentially the same part of the chamber. The contents of the chamber were mixed by two

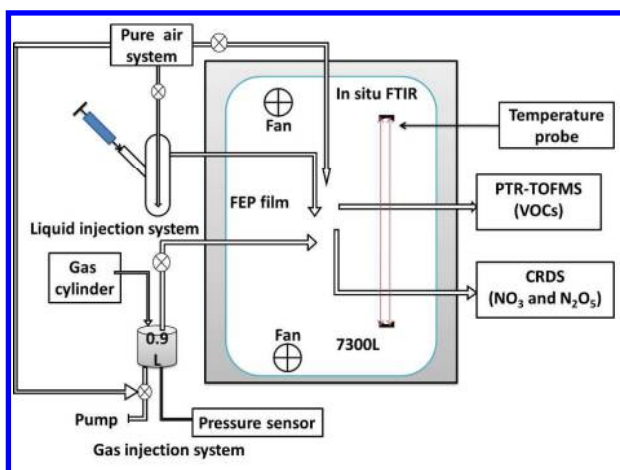
1
2
3
4 125 fans internal to the chamber. In addition, the chamber was equipped with multiple
5
6
7 126 thermocouples to measure temperature and a set of capacitance manometers to measure
8
9
10 127 pressure within the chamber, and a gas handling system to input known amounts of gases
11
12
13 128 into the chamber.

14
15 129 The atmospheric pressure (1000 ± 5 hpa) chamber was made of Teflon film and kept
16
17
18 130 dark by shrouding it in a container equipped with black curtains. Purified dry air (relative
19
20
21 131 humidity $<3\%$) was constantly flowed into the chamber. The chamber was flushed with a
22
23
24 132 large flow (about 120L/min) of dry air to clean out the chamber between experiments or to
25
26
27 133 clean it overnight. However, during kinetics studies, a small flow (about 5-10L/min,
28
29
30 134 depending on the sampling flow rate) of purified air was added just to compensate for the
31
32
33 135 continuous withdrawal of gas from the chamber for analysis; such a flow maintained a
34
35
36 136 constant pressure in the chamber that was slightly above ambient. This flow arrangement
37
38
39 137 resulted in a constant slow dilution of the reactants in the chamber. We measured the
40
41
42 138 dilution rate and mixing time in the chamber by injecting a sample of SF₆ (>99.99%, Alpha
43
44
45 139 Gaz) into the chamber and measuring the temporal profile of SF₆ using the in situ FTIR
46
47
48 140 spectrometer. The mixing time (for near complete mixing, >99%) was about 30 seconds,
49
50
51 141 much shorter than the times for reactions studied here, and the dilution rate could be
52
53
54 142 expressed as a first order rate coefficient of around $2.5\times 10^{-5}\text{s}^{-1}$ (see below).

55 143 The gas handling system, external to the chamber, was designed to inject a known
56
57
58 144 volume of a gas into the chamber. We could also inject a known volume of liquid (that

1
2
3
4 145 evaporated immediately within the chamber) through a septum into a gas flow that reached
5
6
7 146 the middle of the chamber. Pressures in the gas handling system were measured using
8
9
10 147 calibrated capacitance manometers (0-10 and 0-100 Torr, MKS Baratron).

11
12 In the chamber, the organic reactants were detected in real time by using a
13
14
15 149 proton-transfer-reaction time of flight mass spectrometer (PTR-ToF-MS), and the
16
17
18 150 concentrations of N_2O_5 and NO_3 were monitored on line by a two-channel cavity ring down
19
20
21 151 spectrometer (CRDS). The details of these instruments are described in the following
22
23
24 152 sections.



25
26
27
28
29
30
31
32
33
34
35
36
37
38
39
40 153
41
42 154 Figure1: Schematic diagram of the 7300 L chamber used to study the reaction of NO_3 radicals
43
44
45 155 with methacrylate esters along with the analytical methods used to detect reactants. The gas
46
47
48 156 inlet system is shown on the left. The gas outlets and the curtains to keep the chamber dark are
49
50
51 157 not shown. The figure is not to scale.

158 2.1.2 PTR-TOFMS

159 The high-resolution proton-transfer-reaction time-of-flight mass spectrometer
160 (PTR-ToF-MS)¹⁶ (IoniconAnalytik, PTR-ToF-MS 8000) with hydronium ions (H_3O^+) ion
161 source was used to measure methacrylates. The pressure and temperature in the
162 PTR-ToF-MS drift tube was maintained at 2.1 mbar and 333 K. A drift voltage of 400 V
163 was used such that the reduced electric field, E/N , was 98 Td (E is the field strength in V
164 cm^{-1} and N is the number density of gas in molecules cm^{-3}). The flow rate of air from the
165 chamber into the drift tube was approximately 150 mL min^{-1} . The mass resolution of the
166 mass spectrometer, $m/\Delta m$, typically ranged from 3500 to 4500. The mass spectral data
167 were analyzed by a PTR-ToF Data Analyzer software¹⁷ and the normalized peak
168 intensities (in counts per second, ncps) were used for calibration and monitoring. The
169 measured signals varied linearly with the concentrations of the hydrocarbon. The
170 detection sensitivities for the hydrocarbons were derived from the slopes of the
171 calibrations plots of the measured signal (ncps) versus the partial pressure of the
172 hydrocarbon (ppbv) (See also Figure S1 in the supporting information). The detection
173 sensitivities (in units of ncps/ppbv, $1 \text{ ppbv} = 2.46 \times 10^{10} \text{ molecule cm}^{-3}$ at 298K and
174 101.3 kPa) at their monitored mass are shown in Table 1.

175
176 Table 1. A list of specific masses monitored to detect various VOCs using the proton

177 transfer mass spectrometry. The detection sensitivities are also listed.

	Mass charge ratio (m/z)	Detection sensitivities (ncps/ppbv)
propene	43.05	5.22±0.09
propanal	59.5	7.13±0.09
MMA	101.06	38.9±0.5
d8-MMA	109.09	40.0±0.6
EMA	115.07	5.95±0.47
	87.05	39.2±1.7
PMA	87.05	51.4±0.5
IPMA	87.05	46.8±1.4
BMA	87.05	53.8±2.1
IBMA	87.05	26.1±0.5

178

179 2.1.3 CRDS

180 A two-channel cavity ring down spectrometer operating at 662 nm was used to
181 simultaneously measure the concentrations of NO₃ (in one channel) and N₂O₅ + NO₃ (in
182 another channel). The detection principle and operating characteristics of this instrument
183 has been described in detail elsewhere.¹⁸⁻²¹

184 The first channel measured the concentration of NO₃. The second, parallel, channel
185 was heated to convert N₂O₅ to NO₃; total NO₃ (which upon quantitative conversion of
186 N₂O₅ to NO₃) was measured and it represents the sum of NO₃ and N₂O₅. The time
187 resolution of the instrument was 1s with detection sensitivities of between 0.4 and 2 ppt
188 for NO₃ and N₂O₅ for 1 second integration, as described in detail by Fuchs et al.²² The air
189 sample entering the CRDS system was passed through a filter to remove aerosols, which

1
2
3
4 190 scatter the 662 nm light and degrade the instrument sensitivity for gas phase measurement.
5
6
7 191 The combined loss of NO_3 and N_2O_5 to the walls of the instrument and the filter located
8
9
10 192 upstream of this same device have been estimated²²⁻²⁵ to be less than 20% and 4%,
11
12
13 193 respectively, for NO_3 and N_2O_5 ; these losses are accounted for in calculating the
14
15
16 194 concentrations. The uncertainties in the absorption cross section of NO_3 radical at 662 nm
17
18
19 195 and the ratio of the cavity length to the length over which NO_3 and N_2O_5 are present add to
20
21
22 196 the estimated uncertainties. Based on these factors, the overall (asymmetric) accuracy of
23
24
25 197 the NO_3 and N_2O_5 measurements, respectively, are estimated²⁶ to be -8% to +11% and
26
27
28 198 from -9% to +12%. Note that the precision of the measurements of NO_3 and N_2O_5 are
29
30
31 199 much better than the quoted absolute uncertainties under the concentration conditions used
32
33
34 200 in the present study (with initial mixing ratios of NO_3 between 500 and 2,500 pptv and
35
36
37 201 initial mixing ratios of N_2O_5 between 8,000 and 25,000 pptv).

38 39 202 **2.1.4 Fourier Transform Spectrometer**

40
41
42
43 203 A commercial Nicolet 5700 Magna FT-IR spectrometer was coupled to a white-type
44
45
46 204 mirror system located away from the walls and close to the center of the chamber. The
47
48
49 205 optical path length within the chamber was about 140 m. The instrument was operated at a
50
51
52 206 resolution of 1 cm^{-1} . The spectra from the instrument were analyzed using the software
53
54
55 207 provided by the vendor. All the details of the instrument and data analyses are given
56
57
58 208 previously.¹⁴⁻¹⁵ The FTS was used to measure SF_6 (934 cm^{-1} - 954 cm^{-1}), hydrocarbons,

1
2
3
4 209 and some other species during the course of this study; they are noted when appropriate.
5
6

7 8 210 **2.2 Chemicals** 9

10
11 211 The purities of chemicals used in the experiments as given by the manufacturer were:
12
13 212 methyl methacrylate (MMA, > 99%, TCI), ethyl methacrylate (EMA, >99%, TCI), propyl
14
15 213 methacrylate (PMA, >97%, Aldrich), isopropyl methacrylate (IPMA, >98%, TCI), butyl
16
17 214 methacrylate (BMA, >99%, TCI), isobutyl methacrylate (IBMA, >98%, TCI), propene
18
19 215 (>99%, Air Liquid), and propanal (>98%, Aldrich). The isotopic purity of methyl
20
21 216 methacrylate-D8 (MMA-D8 from Apollo Scientific Limited) was quoted to be 99.50
22
23 217 Atom % D. The levels of stabilizers in the samples of esters are noted later. In this study,
24
25 218 the NO₃ radicals were produced by the thermal decomposition of N₂O₅ injected into the
26
27 219 chamber. Pure N₂O₅ was synthesized by mixing NO with O₃ in a slow flow and collecting
28
29 220 N₂O₅ at dry ice temperature, followed by purification, as described by Davidson et al.²⁷
30
31
32
33
34
35
36
37
38
39
40

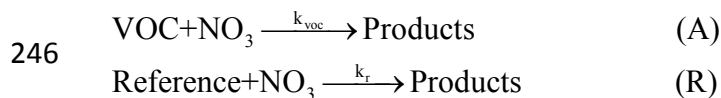
41 221 **2.3 Kinetic study methods and results** 42 43 44

45 222 As noted earlier, we measured the rate coefficients using two different methods: (a) a
46
47 223 relative rate method by following the depletion of a VOC and a reference compound, and
48
49 224 (b) an absolute method where the temporal profiles of NO₃ and N₂O₅ in an excess of VOC.
50
51
52
53 225 For ease of presentation, these two experiments and the obtained results will be presented
54
55
56 226 separately below.
57
58
59
60

227 2.3.1 Relative rate method

228 The experiments were conducted in the chamber (7300L) at atmospheric pressure
229 (1000±5hpa) and at temperature of 298±2K. The depletion of a reactant (each
230 methacrylate esters; hereinafter VOC) and a reference (propene, propanal and MMA) in
231 the presence and in the absence of NO₃ (and N₂O₅ in equilibrium with NO₃ and NO₂) were
232 monitored by PTR-ToF-MS. To account for dilution, as noted earlier, the losses of VOCs
233 in the absence of NO₃ were measured along with the depletion of SF₆ added
234 simultaneously with the VOCs to the chamber. This small decay was essentially first order
235 in the concentrations of VOC and SF₆. The first order rate coefficient for the loss of each
236 reactant in the absence of NO₃ was essentially the same as that for the loss of SF₆; this
237 decay is attributed to dilution caused by the continued injection of dry air into the
238 chamber. The rate first order rate coefficient for the removal of SF₆ and the VOCs, k_d ,
239 was $(2.5 \pm 0.2) \times 10^{-5} \text{ s}^{-1}$. This rate coefficient is essentially what we calculate from the
240 volume flow rates of pure air added to the known volume of the chamber to maintain a
241 constant pressure. The related Figure S2 is given in the supporting information.

242 Subsequent to these measurements, a sample of N₂O₅ was introduced into the
243 chamber where it dissociated to give NO₃. The rates of depletion of VOCs and reference
244 compound were monitored using the PTR-MS. The VOCs and reference compound are
245 competing for the same pool of NO₃ radicals and are represented by the reactions:



247 Under these conditions, their relative losses of the VOC and reference compound are given
248 by:

$$\ln \frac{[\text{VOC}]_0}{[\text{VOC}]_t} - k_d t = \frac{k_{\text{VOC}}}{k_r} \left(\ln \frac{[\text{Reference}]_0}{[\text{Reference}]_t} - k_d t \right) \quad \text{(I)}$$

250 where $[\text{VOC}]_0$ and $[\text{VOC}]_t$ are the concentration of reactant at initial time t_0 and at time t ,
251 $[\text{Reference}]_0$ and $[\text{Reference}]_t$ are the concentration of reactant at t_0 and t , k_{VOC} and k_r were
252 the rate coefficients for reaction (A) and (R), k_d is the first order rate constant for dilution in
253 the chamber. A plot of $\ln([\text{VOC}]_0/[\text{VOC}]_t) - k_d t$ versus $\ln([\text{Reference}]_0/[\text{Reference}]_t) - k_d t$
254 would be a straight line with a zero intercept and a slope of k_{VOC}/k_r . In our experiments, the
255 rate constants of the reactions of the reference compounds with NO_3 radicals were taken
256 to be $k_r(\text{propene}) = (9.5 \pm 5.5) \times 10^{-15} \text{ cm}^3 \text{ molecule}^{-1} \text{ s}^{-1}$, $k_r(\text{propanal}) = (6.3 \pm 2.6) \times 10^{-15}$
257 $\text{ cm}^3 \text{ molecule}^{-1} \text{ s}^{-1}$, $k_r(\text{MMA}) = (2.98 \pm 0.35) \times 10^{-15} \text{ cm}^3 \text{ molecule}^{-1} \text{ s}^{-1}$ (weighted average
258 of the absolute and relative methods from this work; see below). Note that the weighted
259 average for MMA is essentially that measured via the absolute method. The initial
260 concentration of each reactant used in this work is shown in Table 2. A complete
261 summary of the initial concentrations and experimental conditions are given in the
262 supporting information as Table S1.

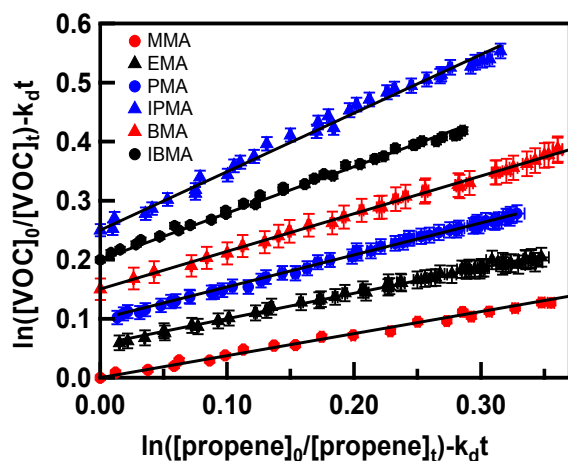
263 Figures 2-1 and 2-2 show the loss of the esters relative to propene and MMA,
264 respectively, according to Equation I. For measurement of each rate constant, several

265 mixtures of the reactant and standard were used and they are all included in the same plots.

266 Clearly, the plots show good linearity for all reactions. These plots were analyzed via

267 linear least squares analyses to obtain the slope of k_{voc}/k_r . The obtained values (average of

268 multiple measurements) of the rate constants are summarized in Table 2.



269

270 Figure 2-1 Plots of the losses of esters relative to those of propene, which was used as the reference.

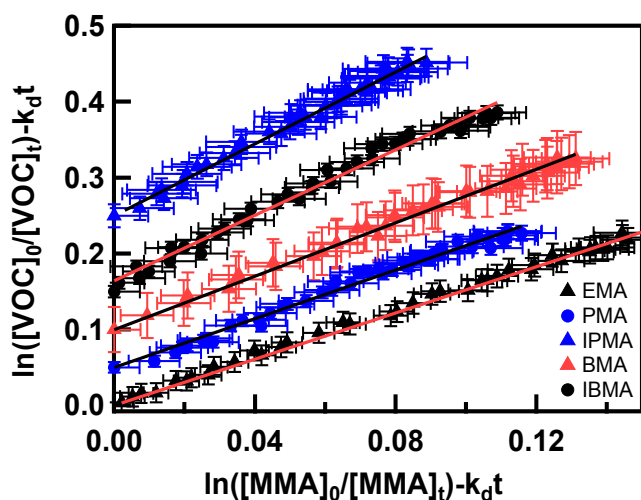
271 The losses shown are for: MMA, red filled circles; EMA, black triangles, Y axis offset by 0.05;

272 PMA, blue filled circles, Y axis offset by 0.1; IPMA, blue triangles, Y axis offset by 0.25; BMA,

273 red triangles, Y axis offset by 0.15; IBMA, black filled circles, Y axis offset by 0.20. The linear

274 least squares fits are shown as lines.

275



276

277 Figure 2-2 Plots of the losses of esters relative to those of MMA used as reference.

278 The specific esters are noted in the legend within the figure (EMA, filled black circles;

279 PMA, blue filled circles, Y axis offset by 0.05; IPMA, blue triangles, Y axis offset by

280 0.25; BMA, red triangles, Y axis offset by 0.1; IBMA, blue filled circles, Y axis

281 offset by 0.15). The linear least squares fits are shown as lines.

282

283 The quoted errors in the rate constant ratios (k_{voc}/k_r) are twice the standard deviation284 ($2\sigma_{k_{\text{voc}}/k_r}$) in the linear least-squares fit of the measured losses to Equation I. In addition to

285 the precision of this ratio, we have included the estimated uncertainty (as given by the

286 IUPAC evaluations) in the rate coefficient ($k_r \pm \sigma_{k_r}$) for the reaction of NO_3 with the

287 reference compound.

288

289 Table 2. Summary of the results from the relative rate study for reaction of NO_3 with

290 methacrylate esters at 298±2K.

VOCs	[VOC] ₀ 10 ¹² (molecule cm ⁻³)	Ref. Compound	No. of experiments	$\frac{k_{voc}}{k_r} \pm 2\sigma_{\left(\frac{k_{voc}}{k_r}\right)}$	$k_{voc} \pm 2\sigma_{voc}$ 10 ⁻¹⁵ (cm ³ molecule ⁻¹ s ⁻¹)
Methyl methacrylate (MMA)	1.13 to 3.40	propene	6	0.37±0.04	(3.52±2.07)
		propanal	2	0.58±0.06	(3.77±1.56)
				Average	(3.6 ₅ ±1.3 ₀)
				Weighted average	(3.6 ₈ ±1.2 ₄)
Ethyl methacrylate (EMA)	1.28 to 2.56	propene	3	0.53±0.05	(5.04±2.95)
		MMA	2	1.55±0.07	(4.62±0.58)
				Average	(4.8 ₃ ±1.5 ₀)
				Weighted average	(4.6 ₃ ±0.5 ₇)
Propyl methacrylate (PMA)	1.10 to 1.66	propene	3	0.56±0.04	(5.32±3.10)
		MMA	3	1.70±0.16	(5.07±0.76)
				Average	(5.2 ₀ ±1.6 ₀)
				Weighted average	(5.0 ₈ ±0.7 ₄)
Isopropyl methacrylate (IPMA)	1.10 to 1.65	propene	3	0.91±0.30	(8.65±5.76)
		MMA	3	2.71±0.61	(8.08±2.05)
				Average	(8.3 ₇ ±3.0 ₆)

				Weighted average	(8.1 ₄ ±1.9 ₃)	
Butyl methacrylate (BMA)	1.01 to 2.53	propene	3	0.70±0.08	(6.65±3.87)	
		MMA	3	1.84±0.12	(5.48±0.74)	
					Average	(6.0 ₇ ±1.9 ₇)
					Weighted average	(5.52±0.72)
Isobutyl methacrylate (IBMA)	0.99 to 2.48	propene	3	0.75±0.02	(7.13±4.13)	
		MMA	3	1.95±0.23	(5.81±0.96)	
					Average	(6.4 ₇ ±2.1 ₂)
					Weighted average	(5.88±0.94)

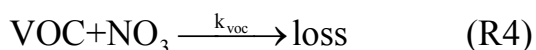
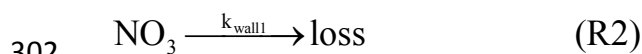
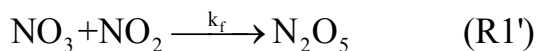
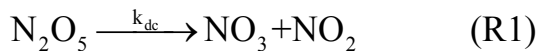
291 The number of appropriate significant figures are shown for the averages. The number of significant
 292 figures in the reported values are more than what is warranted by the errors, but are shown for
 293 completeness. To maintain consistent number of significant figures, some numbers with larger errors are
 294 shown with the last digit as a subscript.

295 **2.3.2 Rate coefficients via monitoring temporal profiles of NO₃/N₂O₅ loss using**

296 **CRDS**

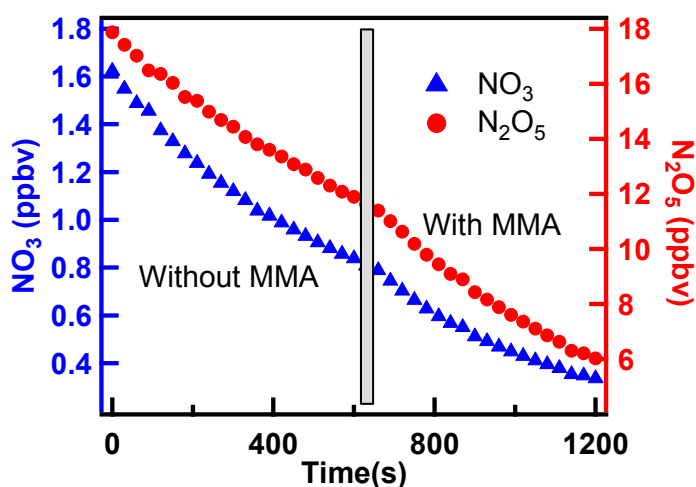
297 The rate coefficients for the reactions of NO₃ radicals with methacrylate esters were
 298 also measured by following the temporal profiles of NO₃ and N₂O₅ in an excess of esters.
 299 During this process, NO₃ and N₂O₅ are nearly in equilibrium such that one could simply

300 attempt to fit the temporal profiles to obtain the rate coefficients. However, we fitted the
 301 observed profiles to the following set of reactions that occur in the chamber:



303 First, N_2O_5 was injected into the middle of the chamber. N_2O_5 decomposed
 304 immediately in the chamber to give NO_3 and NO_2 and set up an equilibrium with remaining
 305 N_2O_5 . The temporal variation of NO_3 and N_2O_5 in the chamber were continuously
 306 measured using CRDS. The concentrations of NO_3 and N_2O_5 decreased with time as N_2O_5
 307 and NO_3 were lost in the chamber due to wall loss and reaction with impurities.

308



309

310 Figure 3 Measured temporal profiles of NO_3 and N_2O_5 mixing ratios in the chamber in the

311 absence (up to the vertical gray bar) and presence of MMA (after the gray bar). The gray bar

1
2
3
4 312 indicates the time at which VOCs were injected into the chamber and the time it took for
5
6
7 313 complete mixing. $k_{\text{wall1}}=0.0065 \text{ s}^{-1}$, $k_{\text{wall2}}=0.00032 \text{ s}^{-1}$.
8
9

10 314

11
12 315 Typical observed temporal profiles of NO_3 and N_2O_5 in such experiments after
13
14
15 316 injection of N_2O_5 into the chamber are shown in Figure 3. The measured temporal profiles
16
17
18 317 were fit using a box model that integrated the set of reactions shown above to derive the
19
20
21 318 time dependence of NO_3 and N_2O_5 . The fitting was done by minimizing the sum of least
22
23
24 319 squares for both NO_3 and N_2O_5 profiles, by changing the input parameters that included
25
26
27 320 wall loss rates, the equilibrium constant, the rate coefficient for the reaction of NO_3 with
28
29
30 321 VOC as well as the initial NO_2 concentration. First, the data in the absence of VOC was
31
32
33 322 fit to the reaction scheme with VOC concentration set to zero. Using the known values of
34
35
36 323 the rate coefficients for Reactions R1 and R1', the values of k_{wall1} , k_{wall2} , and the initial
37
38
39 324 concentration of NO_2 were derived from the fit. The equilibrium constant was slightly
40
41
42 325 varied to improve the fit, if necessary. The first-order wall loss rate constants of NO_3 and
43
44
45 326 N_2O_5 , respectively, $k_{\text{wall1}} (\text{s}^{-1})$ and $k_{\text{wall2}} (\text{s}^{-1})$. Note that we did not have an accurate
46
47
48 327 independent measure of NO_2 in the chamber since our NO_2 detector (which converted NO_2
49
50
51 328 to NO by passing it over a hot molybdenum catalyst) also detected N_2O_5 . Occasionally, we
52
53
54 329 needed to change the N_2O_5 dissociation rate constant by at most 10% to improve the fit,
55
56
57 330 which reflected the uncertainty in the temperature in the chamber of about 1 K. The
58
59
60 331 equilibrium constant, $k_{\text{eq}} = [\text{N}_2\text{O}_5]/[\text{NO}_3][\text{NO}_2] = k_f/k_{\text{dc}}$, and value of k_{dc} , k_{eq} and k_f at

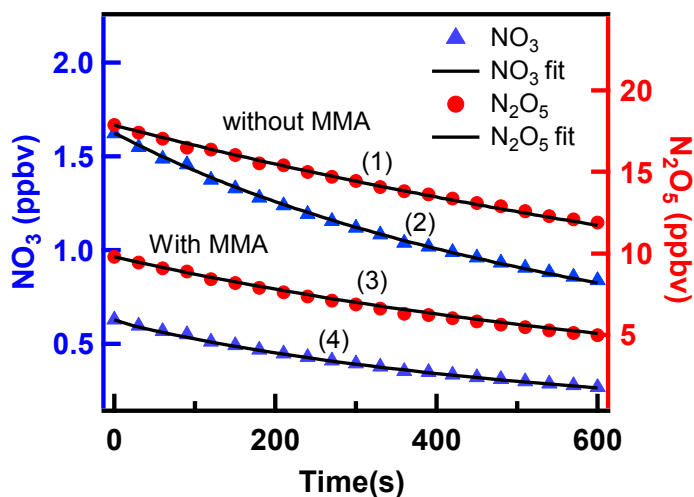
1
2
3
4 332 different temperature were taken from NASA/JPL recommendation.²⁹
5
6

7 333 After about 10 minutes, a sufficient length of time for NO₃ and N₂O₅ observations that
8
9 334 enabled an accurate calculation of the equilibrium constant, a known concentration of the
10
11 335 VOC was introduced into the chamber and its concentration was measured using PTR-MS
12
13 336 and/or FTIR instruments. The concentration of the ester was always much greater than
14
15 337 those of N₂O₅ or NO₃ in the chamber. The temporal profile of N₂O₅ and NO₃ measured
16
17 338 after 60 s of VOC injection were again fit to minimize the sum of least squares for NO₃ and
18
19 339 N₂O₅ decays in the above reaction scheme with only the rate coefficient for the reaction of
20
21 340 VOC with NO₃ being the variable As noted earlier, the time for complete mixing was 30 s.
22
23 341 The initial concentration of NO₂ was taken to be equal to that calculated just prior to adding
24
25 342 the VOC assuming equilibrium between NO₃ and N₂O₅, i.e.,
26
27
28
29
30
31
32
33

34
35 343
$$[\text{NO}_2]_0 = \frac{[\text{N}_2\text{O}_5]_0}{[\text{NO}_3]_0 k_{\text{eq}}} \quad (\text{II})$$

36
37
38

39 344 Figure 4 shows a fit of the observed temporal profiles of NO₃ and N₂O₅ and the fit of the
40
41 345 profiles to the above reaction scheme.
42
43
44
45
46
47
48
49
50
51
52
53
54
55
56
57
58
59
60



346

347 Figure 4: Observed NO_3 and N_2O_5 mixing ratios (circles and triangles) and their simulated348 temporal profiles (lines) after the injection of VOC into the chamber where NO_3 and N_2O_5 were349 present at equilibrium. Profile (1) - loss of N_2O_5 without MMA; Profile (2) - loss of NO_3 350 without MMA; Profile (3) - loss of N_2O_5 with MMA; Profile (4) - loss of NO_3 with MMA.351 The concentration of MMA was 3.06×10^{12} molecule cm^{-3} . The fits yield a value of $k_{\text{voc}} =$ 352 2.98×10^{-15} molecule $^{-1}$ cm^3 s^{-1} .353 Multiple experiments were carried out by varying VOC and initial N_2O_5 354 concentrations. In some cases, we included additional NO_2 in the chamber before the355 addition of N_2O_5 (to shift the equilibrium). The uncertainty in obtained value of $k(\text{VOC})$

356 due to fitting was very small, often much less than 3 %. However, the fits alone do not

357 determine the uncertainty in the precision of our measured rate coefficient. They were

358 obtained the standard deviation of the mean of multiple measurements and including the

359 Student t value for the limited number of measurements. The results of our measurements

360 are given in Table 3.

361

362

Table 3. Summary of the experimental conditions for and results from the absolute

363

method to measure the rate constants for reaction of NO₃ with VOCs at 298±2K. The

364

k_{VOC} values shown are those derived from fitting the observed profiles of NO₃ and

365

N₂O₅ to a least squares algorithm.

Compound	T (K)	Initial mixing ratio (ppbv)			k _{VOC} measured ^a	k _{VOC} incl. systematic errors ^b
		VOC	NO ₃	N ₂ O ₅	10 ⁻¹⁵ (cm ³ molecule ⁻¹ s ⁻¹)	
Propene	296	156.6	0.54	10.16	9.15	
	296	70.0	0.45	9.77	9.97	
					(9.56±1.36)	(9.56±1.80)
MMA	295	121.9	0.68	11.05	2.90	
	296	124.3	0.63	9.79	2.98	
	298	363.7	0.78	11.46	2.89	
					(2.92±0.12)	(2.92±0.37)
EMA	298	126.1	0.81	10.85	4.56	
	300	130.1	0.59	6.79	5.09	
	298	333.3	1.13	16.58	4.69	
					(4.78±0.65)	(4.78±0.93)

PMA	297	113.5	0.79	11.15	5.14	
	300	279.7	1.11	10.13	5.77	
	296	113.6	0.83	8.33	5.59	
					(5.50±0.76)	(5.50±1.00)
IPMA	297	101.6	0.81	10.28	7.94	
	296	86.2	0.91	13.01	7.56	
	300	209.3	0.84	13.69	8.00	
					(7.83±0.56)	(7.83±1.15)
BMA	299	264.2	1.00	8.80	6.16	
	299	199.2	1.25	11.42	5.86	
	300	251.8	1.10	12.92	6.00	
					(6.00±0.35)	(6.00±0.89)
IBMA	296	142.3	0.77	10.90	6.52	
	297	154.5	1.09	13.00	6.46	
	297	162.6	0.99	9.44	6.82	
					(6.60±0.45)	(6.60±0.94)

366 ^a Quoted error is at the 95% confidence level and is a measure of the precision of our measurements. It
 367 includes Student t-distribution contribution due to the limited number of measurements. To maintain
 368 consistent number of significant figures, some numbers with larger errors are shown with the last digit as

1
2
3
4 369 a subscript.
5
6

7 370 ^b The quoted errors include estimated systematic errors as described in the text.
8
9

10 371
11
12

13 372 **2.4 Error estimation**

14
15
16

17 373 *Relative rate measurements:* One of the advantages of relative rate measurements is that
18
19
20 374 uncertainties in absolute concentrations of either reactant do not lead to an error in the
21
22
23 375 measured values since we depend on the relative concentrations changes as the reaction
24
25
26 376 proceeds to derive the rate constant. The concentrations of the reactant, in our case esters,
27
28
29 377 and the reference compound (propene, propanal, or MMA) were measured using the same
30
31 378 PTR-ToF-MS system. The calibration plots of the concentration of VOC versus their
32
33
34 379 signals were linear. The precision of the measured signal contributes to the precision of
35
36
37 380 the measured rate constants. The slopes of the plots shown in Figures 2-1 and 2-2 yielded
38
39
40 381 the precision of the measurement. The errors in the values of rate constant ratios (k_{voc}/k_r)
41
42
43 382 are twice the standard deviation ($2\sigma_{k_{\text{voc}}/k_r}$) in the least-squares fit of the measured losses to
44
45
46 383 Equation I. In addition to the precision, the main contributor to the accuracy of the
47
48
49 384 measured rate constant is the accuracy of the rate coefficients for the reference reactions.
50
51 385 The rate coefficient for the reactions of NO_3 with propene and propanal have been
52
53
54 386 evaluated and we assume the accuracy to be those assessed by the evaluation panels,
55
56 387 $k_r(\text{propene})^{28} = (9.5 \pm 5.5) \times 10^{-15} \text{ cm}^3 \text{ molecule}^{-1} \text{ s}^{-1}$, $k_r(\text{propanal})^{28} = (6.3 \pm 2.6) \times 10^{-15} \text{ cm}^3$
57
58
59
60

1
2
3
4 388 molecule⁻¹s⁻¹. (As noted later, we believe that the uncertainty for the reaction of NO₃ with
5
6
7 389 propene is less than that noted by the evaluation.) We combined the precision of our
8
9
10 390 measured values with the quoted uncertainties in the rate coefficient for the reference
11
12
13 391 reaction to estimate the overall accuracy of the measured rate coefficients.

14
15
16
17 392
$$\sigma_{\text{voc}} = k_{\text{voc}} \sqrt{\left[\frac{2\sigma_{\left(\frac{k_{\text{voc}}}{k_r}\right)}}{\frac{k_{\text{voc}}}{k_r}} \right]^2 + \left[\frac{\sigma_{k_r}}{k_r} \right]^2} \quad (\text{III})$$

18
19
20
21

22 393 *Absolute rate constant measurements*- The errors in determining the rate coefficients by
23
24 394 monitoring the temporal profiles of NO₃ and N₂O₅ arise from the precision in the
25
26
27
28 395 measurements of NO₃ and N₂O₅, the absolute values of N₂O₅ and NO₃ and the uncertainty
29
30
31 396 in the concentration of the excess reagent, the esters in our study. Ordinarily, the absolute
32
33
34 397 values of the NO₃ reactant would not be needed in an absolute method where NO₃ temporal
35
36
37 398 profile is monitored in an excess of esters. However, in the present study, NO₃ is in
38
39 399 equilibrium (or almost in equilibrium) with N₂O₅ and this situation requires absolute
40
41
42 400 concentrations of the NO₃ and N₂O₅. The systematic errors in measurements of NO₃ and
43
44
45 401 N₂O₅ using the CRDS system employed here have been assessed to be -8/+11% for NO₃
46
47
48 402 and -9/+12% for N₂O₅, as noted earlier. The uncertainty in the fitting, as noted above, is
49
50
51 403 better than 3%. Systematic errors in the measured concentration of the esters are estimated
52
53
54 404 for each compound using the uncertainty of the slope in the calibration plots (<4%) and the
55
56 405 uncertainty in measuring ester concentration for the calibration (5%); all at 95%
57
58
59
60

1
2
3
4 406 confidence level. We just added these two errors to get the estimated uncertainty in the
5
6
7 407 concentration of esters in the chamber since they could be correlated. Then, the overall
8
9
10 408 estimated error was calculated by adding in quadrature the fitting error, estimated
11
12
13 409 contribution of absolute concentrations of NO_3 and N_2O_5 , the precision of the
14
15
16 410 measurements of k_{VOC} , and the estimated uncertainty in the concentration of the esters.
17
18 411 Table 3 lists the uncertainties in the measured values of the rate constants along with the
19
20
21 412 estimated systematic errors.
22

23
24 413 We measured the rate coefficient for the reaction of NO_3 with propene using the
25
26
27 414 absolute method. Our obtained results are in very good agreement with most of the
28
29
30 415 literature values. This adds further confidence in our measured values of the rate
31
32
33 416 coefficients using the absolute method. We note that most of the reported values for the
34
35
36 417 rate coefficient for the NO_3 reaction with propene in the IUPAC assessment appears to
37
38
39 418 agree reasonably well, though there are a few outliers. We suggest that the error bars given
40
41
42 419 for the reaction of NO_3 with propene in the IUPAC is excessively conservative.
43

44 420 Another potential source of error in the rate coefficient measured using the absolute
45
46
47 421 method is presence of reactive impurities in the sample of the esters. The methacrylates
48
49
50 422 used in the study were the purest we could obtain from commercial vendors (see materials
51
52
53 423 section for purity levels). However, they contained some stabilizers, which could
54
55
56 424 potentially react more rapidly with NO_3 than the esters. The stabilizers used in the
57
58
59 425 methacrylates were normally around 10-20 ppmv, the maximum was about 200 ppmv of
60

1
2
3
4 426 4-Methoxyphenol (MEHQ) in isopropyl methacrylate (IPMA). Stabilizers used with these
5
6
7 427 esters are aromatic compounds with a large side chain containing a saturated group. If
8
9
10 428 MEHQ reacted very rapidly with NO_3 , we could indeed overestimate this rate coefficient.
11
12 429 Indeed, if the rate coefficient for the reaction of MEHQ with NO_3 were $1 \times 10^{-10} \text{ cm}^3$
13
14
15 430 $\text{molecule}^{-1} \text{ s}^{-1}$ as quoted for other methoxyphenols by Lauraguais et al.³⁰ we should have
16
17
18 431 measured a value of roughly $2 \times 10^{-14} \text{ cm}^3 \text{ molecule}^{-1} \text{ s}^{-1}$ for IPMA. However, our measured
19
20
21 432 values using the direct and relative methods agree well (see Table 4). Therefore, we do not
22
23
24 433 believe that our reported values were greatly affected by the presence of MEHQ. In case of
25
26
27 434 the other esters, the presence of stabilizers at the quoted levels would contribute at most 20%
28
29
30 435 to the measured value using the direct method. Again, the agreement between the relative
31
32
33 436 and direct method suggests that the contributions of the stabilizer to the measured rate
34
35
36 437 coefficients were not large. We note that the PTR-ToF-MS spectra of each of the esters did
37
38
39 438 not show any measurable hydrocarbons other than the ester. Based on these observations,
40
41
42 439 we conclude that our measured absolute rate coefficients were not significantly influenced
43
44
45 440 by the presence of impurities.

46 441 Lastly, we note that the rate coefficients measured here reflect that for the reaction of
47
48
49 442 NO_3 with esters and there is no significant contribution from any possible reaction of N_2O_5
50
51
52 443 with esters. First, we varied the ratio of NO_3 to N_2O_5 by changing NO_2 and the measured
53
54
55 444 rate coefficients were insensitive to this ratio. Second, the rate coefficients measured using
56
57
58 445 the absolute method agrees with that from the relative method, where some of the reference

1
2
3
4 446 molecules are known to be non-reactive towards N_2O_5 . Again, in these experiments, the
5
6
7 447 ratios of NO_3 to N_2O_5 were very different and it also varied with the extent of reaction, with
8
9
10 448 no effect on the derived rate coefficients.

11
12
13 449

14 15 16 450 **3 Discussion**

17 18 19 20 451 **3.1 Comparison of rate coefficients obtained from two methods**

21
22
23
24 452 We used two different methods to measure the rate coefficients for the reactions of
25
26
27 453 NO_3 with methacrylate esters; they are summarized in Table 4. The rate constants values
28
29
30 454 we measured using the two methods are in good agreement with each other, given the
31
32
33 455 estimated uncertainties in the rate constants. The largest difference is for the reaction of
34
35
36 456 NO_3 with MMA, where the rate coefficients from the two methods differ by about 25%.

37
38 457 We have used weighted average of the two methods, i.e., the absolute and the relative
39
40
41 458 rate methods, to derive the best possible values for the rate coefficients for the reactions
42
43
44 459 of NO_3 with methacrylate esters studies here. They are shown in Table 4.

45
46
47 460

48
49 461 Table 4 Rate constants values obtained in two methods for the reactions of NO_3 with
50
51
52 462 methacrylate esters.

	Rate constants $k_{\text{voc}}(10^{-15})$	Ratio	k_{voc}
--	---	-------	------------------

	molecule ⁻¹ cm ³ s ⁻¹)		(k _{rm} /k _{ab})	(10 ⁻¹⁵ molecule ⁻¹ cm ³ s ⁻¹)	
	Relative method (k _{rm})	Absolute method (k _{ab})		Unweighted average	Weighted average
MMA(k ₁)	(3.68±1.24)	(2.92±0.37)	1.26	(3.30±0.65)	(2.98±0.35)
EMA(k ₂)	(4.63±0.57)	(4.78±0.93)	0.97	(4.70±0.55)	(4.67±0.49)
PMA(k ₃)	(5.08±0.74)	(5.50±1.00)	0.92	(5.29±0.62)	(5.23±0.60)
IPMA(k ₄)	(8.14±1.93)	(7.83±1.15)	1.04	(7.9 ₉ ±1.1 ₂) ^a	(7.9 ₁ ±1.0 ₀) ^a
BMA(k ₅)	(5.52±0.72)	(6.00±0.89)	0.92	(5.76±0.57)	(5.71±0.56)
IBMA(k ₆)	(5.88±0.94)	(6.60±0.94)	0.89	(6.24±0.66)	(6.24±0.66)

463 a. To maintain consistent number of significant figures, some numbers with larger errors are shown with the
 464 last digit as a subscript.

465

466 Indeed, one could opt to use an unweighted average. Therefore, we have also listed them
 467 in the table. We prefer the weighted average mostly to put more weight on the direct
 468 method, especially since the quoted uncertainty in the rate coefficient for the reaction of
 469 NO₃ with propene, a common reference for relative rate studies, is unusually large. This
 470 is discussed later.

471 **3.2 Comparison with the kinetic results in literature**

472 Several groups have measured the rate constants of NO₃ radical reactions with MMA,
473 EMA and BMA using relative methods in small chambers (<150L) at room temperature
474 and atmospheric pressure. In their experiments, the initial mixing ratios of the
475 methacrylate esters were in a range of 5-20ppmv. A comparison of rate coefficients
476 determined in this study with the literature data is shown in Table 5. As can be seen in the
477 table, our values are in good agreement with previously reported values, given the reported
478 uncertainties, whenever such comparisons are possible.

479 Given the reasonably good agreement between various reported studies and a lack of
480 obvious reasons to prefer one study over the other, we suggest that an un-weighted average
481 of all the results be used as recommended values for the rate coefficient. Such average
482 values are also reported in the Table 5. Clearly, there are no previous reports for the rate
483 coefficients for the reactions of NO₃ with PMA, IPMA, and IBMA. However, given the
484 similarities of those compounds with the other methacrylates studied here, it appears that
485 our rate coefficients are also accurate to about 20% and could be used with confidence.

486

487

488 Table 5 Summary of the rate coefficients of NO₃ with MMA, EMA and BMA obtained
489 from literatures and this work.

Reactant	Reference Chemical	k_{VOC} reported $10^{-15} \text{ cm}^3 \text{ molecule}^{-1} \text{ s}^{-1}$	Reference
MMA	propene	$(3.7_1 \pm 2.2_2)^a$	10
	propene	$(3.5_1 \pm 2.0_4)^a$	12
	propene	$(3.6_1 \pm 2.1_0)^a$	13
	propene	$(3.5_2 \pm 2.0_7)$	This work
	methacrolein	$(3.5_1 \pm 1.0_8)$	13
	1-butene	$(3.7_2 \pm 1.1_5)$	12
	propanal	$(3.7_7 \pm 1.5_6)$	This work
	AM ^b	(2.92 ± 0.37)	This work
		(3.12 ± 0.31)	Weighted average of all work
		(3.53 ± 0.60)	Unweighted average of all work
EMA	propene	$(4.8_1 \pm 2.8_0)^a$	12
	propene	$(5.7_0 \pm 3.3_1)^a$	13
	propene	(5.04 ± 2.95)	This work
	1-butene	$(5.0_9 \pm 1.6_1)$	12
	methacrolein	$(5.1_6 \pm 1.5_9)$	13
	MMA	(4.62 ± 0.58)	This work
	AM ^b	(4.78 ± 0.93)	This work

		(4.76±0.44)	Weighted average of all work
		(5.03±0.83)	Unweighted average of all work
BMA	propene	(8.2 ₇ ±4.8 ₃) ^a	13
	propene	(6.6 ₅ ±3.8 ₇)	This work
	1-butene	(7.5 ₈ ±4.3 ₆)	13
	MMA	(5.48±0.74)	This work
	AM ^b	(6.00±0.89)	This work
		(5.78±0.55)	Weighted average of all work
		(6.8 ₀ ±1.5 ₃)	Unweighted average of all work
PMA		(5.23 ± 0.60)	This work
IPMA		(7.9 ₁ ±1.0 ₀)	This work
IBMA		(6.24±0.66)	This work

490 ^a The values from the literatures were recalculated by using the rate constant of propene with NO₃ (9.5
 491 ± 5.5) × 10⁻¹⁵ cm³ molecule⁻¹s⁻¹, which was used in our study. Note that these uncertainties are likely to
 492 be overestimated because of the large uncertainty quoted by IUPAC. To maintain consistent number of
 493 significant figures, some numbers with larger errors are shown with the last digit as a subscript.

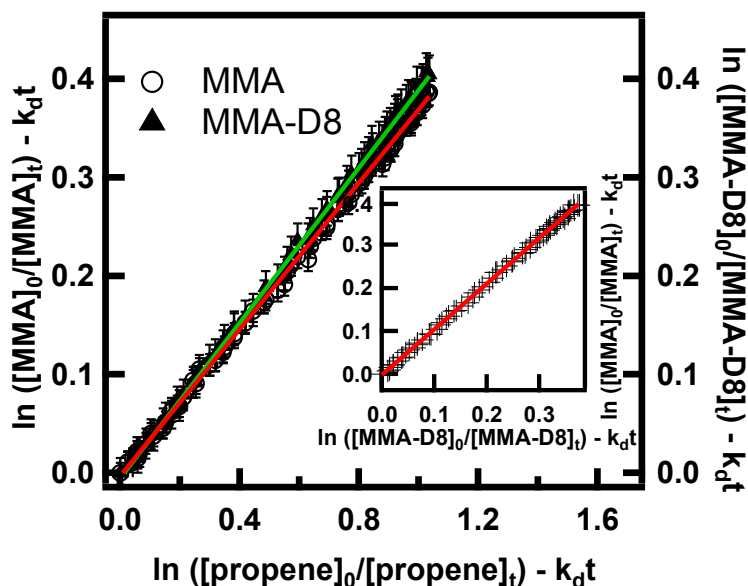
494 ^b Measured from the temporal profiles of NO₃ and N₂O₅, referred to as the absolute method.

1
2
3
4 495 **3.3 Mechanism and Relationship between structure and reactivity of the**
5
6
7 496 **methacrylate esters**
8
9

10
11 497 The rate coefficients for all the methacrylate measured here are roughly in the same
12
13 498 range, with the rate coefficient slightly increasing with extent of substitution going from
14
15
16 499 methyl to ethyl to propyl to butyl methacrylate. We observe an increase in the reactivity
17
18
19 500 with the chain length of the alkyl group. $k_{\text{voc}}(\text{MMA}) < k_{\text{voc}}(\text{EMA}) < k_{\text{voc}}(\text{PMA}) < k_{\text{voc}}(\text{BMA})$.
20
21
22 501 Further, the isoalkyl methacrylates react a little faster than their normal analogs. This is
23
24
25 502 consistent with the electron donating inductive effect of the substituents ($-\text{C}(\text{O})\text{OR}$),
26
27 503 consistent with an electrophilic addition mechanism.³¹ Such variations are consistent with
28
29
30 504 NO_3 reaction proceeding via electrophilic addition to the double bond in the methacrylate
31
32
33 505 group. These rate constants that have been measured for unsaturated esters, help
34
35
36 506 understand the structure activity relationship (SAR) and complete the parameterization of
37
38
39 507 this family of compounds. We have refrained from calculating SAR relations till data is
40
41
42 508 available for esters. Curiously, however, the isopropyl methacrylate reacts faster than the
43
44
45 509 normal analog while the isobutyl methacrylate reacts with almost the same rate
46
47
48 510 coefficient as the butyl methacrylate. It would be interesting to see if there is enhanced H
49
50
51 511 abstraction in IPMA reaction and leads to HNO_3 as a product.

52
53 512 To further examine this mechanism for the reaction, we studied the reaction of NO_3
54
55
56 513 with deuterated MMA. The rate coefficients for the reactions of MMA and MMA-D8 with
57
58
59
60

514 NO_3 radicals are essentially identical, with $k_H/k_D = 0.98$, as shown in Figure 5. The
 515 isotopic purity of the MMA-D8 was high (>99%); therefore, this equality is not due to
 516 the deuteration being insufficient. The observed equality of the rate coefficients for the
 517 deuterated and non-deuterated MMA further strengthens the expectation that H atom
 518 abstraction is insignificant in the reaction of NO_3 with methacrylates.

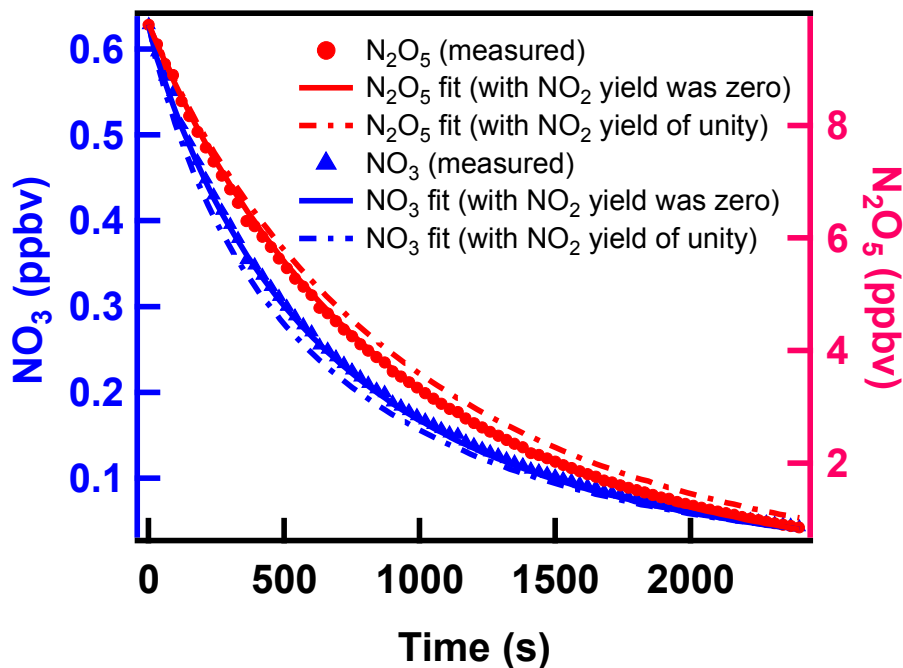


519
 520 Figure 5: The rates of losses of MMA-D8 relative to those for propene while competing for the same
 521 pool of NO_3 radicals. The green line is a fit to the MMA-D8 and the red line is a fit to the MMA data. The
 522 inset shows a similar plot for the loss of MMA relative that for MMA-D8, with a slope of essentially
 523 unity showing the both deuterated and non-deuterated MMA react with NO_3 with the same rate
 524 coefficient, i.e., $k_1 \approx k_7$.

525 Furthermore, in our experiments, we deduced NO_2 was not produced after NO_3 was
 526 removed. Figure 6 shows the observed NO_3 and N_2O_5 profiles in the presence of MMA.
 527 Simulation of these profiles where we include a yield of NO_2 of unity is shown as the

1
2
3
4 528 dashed line. Clearly, we cannot fit the data to a scheme where NO_2 is produced from the
5
6
7 529 reaction with a large yield. If NO_2 were the product of the reaction, we would expect a
8
9
10 530 production of one NO_2 for each NO_3 lost, unless there is stoichiometric removal of NO_2
11
12
13 531 by a peroxy radical formed by the NO_3 reaction with the methacrylate ester that reacts
14
15 532 very rapidly with NO_2 to form a stable nitrate. Since, we cannot rule out the formation of
16
17
18 533 such a nitrate, we cannot unequivocally rule out the formation of NO_2 as a product of the
19
20
21 534 reaction. Future studies in a chamber that were constrained by an accurate measurements
22
23
24 535 of NO_2 and total NO_y would be useful in constraining the branching ratio toward NO_2 or
25
26
27 536 organic nitrate production, even if the former were small. Similarly, a simulation of the
28
29
30 537 all the subsequent reactions would be useful when the majority of the stable products are
31
32 538 identified and quantified.

33
34
35 539
36
37
38
39
40
41
42
43
44
45
46
47
48
49
50
51
52
53
54
55
56
57
58
59
60



540

541 Figure 6 Experimental and simulated results for NO_3 and N_2O_5 profiles from chamber experiment542 (MMA+ NO_3) when NO_2 was set as a product of unit yield in the modeled reaction scheme.

543 Based on these observation we suggest that, the atmospheric oxidation mechanism

544 of NO_3 reactions with unsaturated carbonyl group compounds proceeds mostly via

545 electrophilic addition to the C=C double bond.

546

3.4 Atmospheric implication

547 Once emitted into the atmosphere, the studied methacrylate esters are removed

548 mainly through their reactions with reactive species such as OH, NO_3 , O_3 and chlorine

549 atoms. The lifetimes for the removal of the esters were calculated using nominal

550 concentrations of the reactive radicals and ozone in the lower troposphere. Note that these

551 lifetimes are nominal values and are expected to be location and time dependent. The

lifetimes were calculated using the equation:

$$\tau = \frac{1}{k_{\text{voc+x}} [\text{X}]} \quad (\text{IV})$$

where $k_{\text{voc+x}}$ is the rate coefficient for the reaction of the oxidant with the methacrylate ester and $[\text{X}]$ is the nominal representative atmospheric concentration of the oxidants.

Tropospheric concentrations of OH, NO₃, O₃ and chlorine atoms that could be expected were used in the calculations to approximate the loss of esters in the troposphere. Here we take their concentrations to be: $[\text{Cl}] = 1 \times 10^4 \text{ molecule cm}^{-3}$ ³², $[\text{OH}] = 1 \times 10^6 \text{ molecule cm}^{-3}$ ³³, $[\text{NO}_3] = 5 \times 10^8 \text{ molecule cm}^{-3}$ ³⁴, $[\text{O}_3] = 1 \times 10^{12} \text{ molecule cm}^{-3}$ (~40 ppbv). Note that NO₃ concentration in locations where esters are emitted (such as urban plumes) can be much larger³⁵. However, the lifetimes would still be many days such that the esters would be dispersed. Therefore, the calculated atmospheric lifetimes of the methacrylate esters summarized in Table 6 would be reasonably representative of the removal processes for these esters.

The atmospheric lifetimes for methacrylate esters due to reaction with OH radicals are roughly a few hours, followed by that due to loss via reaction with ozone of ~40 hours. Clearly, the reaction of NO₃ would contribute only about 5% to the overall lifetime. However, in dark areas with large NO_x emissions, the loss via reaction with NO₃ could be significant compared to that via reaction with OH. However, the abundances of NO₃ are closely related to those of O₃ since it is formed by the reaction of NO₂ with O₃.

1
2
3
4 571 Therefore, clearly, both the reaction of O_3 and NO_3 will contribute significantly at night
5
6
7 572 when the NO_x emissions are high.
8
9
10
11
12
13
14
15
16
17
18
19
20
21
22
23
24
25
26
27
28
29
30
31
32
33
34
35
36
37
38
39
40
41
42
43
44
45
46
47
48
49
50
51
52
53
54
55
56
57
58
59
60

573 Table 6. Summary of rate constants and estimated atmospheric lifetimes of methacrylate esters with respect to their reactions with
 574 OH, NO₃, O₃ and Cl at (298±2)K and atmospheric pressure.

	Rate constants (cm ³ molecule ⁻¹ s ⁻¹)				Lifetime (hours)			
	k _{OH}	k _{NO₃}	k _{O₃}	k _{Cl}	τ _{OH}	τ _{NO₃}	τ _{O₃} ⁱ	τ _{Cl}
MMA	(4.2)×10 ⁻¹¹ [b,c,d]	(2.98)×10 ⁻¹⁵ [a]	(7.51)×10 ⁻¹⁸ [d]	(2.17)×10 ⁻¹⁰ [f]	6.6	186	37	128
EMA	(4.58)×10 ⁻¹¹ [c]	(4.67)×10 ⁻¹⁵ [a]	(7.68)×10 ⁻¹⁸ [e]	(2.71)×10 ⁻¹⁰ [f]	6.1	119	36	103
PMA		(5.23)×10 ⁻¹⁵ [a]				106	~40	
IPMA		(7.91)×10 ⁻¹⁵ [a]				70	~40	
BMA	(7.08)×10 ⁻¹¹ [c]	(5.71)×10 ⁻¹⁵ [a]		(3.72)×10 ⁻¹⁰ [f,g]	3.3	97	~40	75
IBMA		(6.24)×10 ⁻¹⁵ [a]				89	~40	

575 Assuming [OH] = 1×10⁶ molecule cm⁻³,³³ [NO₃] = 5×10⁸ molecule cm⁻³,³⁴ [O₃] = 1×10¹² molecule cm⁻³ (~40 ppbv), and [Cl] = 1×10⁴ molecule cm⁻³.³²

1
2
3
4
5
6 576 a This work.
7

8
9 577 b,c,d are from references 3, 4, and 5: Value reported by ref. d is roughly a factor of 2 lower than that reported by ref. b and c. We used the average value from ref. b
10

11 578 and c.
12

13
14 579 e from reference 7, f from reference 36, and g from reference 9.
15

16
17 580 i. When the rate coefficients for the reactions of esters with ozone were not available, we have assumed it to be roughly the same as that for MMA.
18
19
20
21
22
23
24
25
26
27
28
29
30
31
32
33
34
35
36
37
38
39
40
41
42
43
44
45
46
47
48
49

1
2
3
4
5 581 **Supporting Information.**
6
7

8
9 582 Table S1-S2, a complete summary of the initial concentrations and experimental
10
11 583 conditions for the relative rate method and absolute rate methods; Figure S1, Calibration
12
13 584 of each reactants and references in PTR-ToF-MS; Figure S2, the first order decay rate of
14
15 585 SF₆ and MMA in the absence of NO₃; Figure S3, experimental and simulated results for
16
17
18
19
20 586 NO₃ and N₂O₅ profiles from absolute rate method experiments.
21
22

23
24 587
25
26
27

28 588 **Acknowledgments**
29
30

31
32 589 This work was supported by Labex Voltaire (ANR-10-LABX-100-01) and ARD PIVOTS
33
34 590 program (supported by the Centre-Val de Loire regional council). ARR's work was
35
36
37 591 supported by Colorado State University. ARR and SSB are grateful to Prof. Veronica Vaida
38
39
40 592 for her exquisite science and for being a wonderful colleague and a friend over many
41
42
43 593 decades. It is our pleasure to be a part of her Festschrift.
44
45

46 594
47
48

49
50 595 **References**
51
52

53
54 596 1. European Union. Risk Assessment. methyl methacrylate. Bundesanstalt für
55
56
57 597 Arbeitsschutz und Arbeitsmedizin. 2002.
58
59
60

- 1
2
3
4 598 2. Mellouki, A.; Le Bras, G.; Sidebottom, H., Kinetics and mechanisms of the oxidation
5
6
7 599 of oxygenated organic compounds in the gas phase. *Chem. Rev.* **2003**, *103* (12),
8
9
10 600 5077-5096.
- 11
12 601 3. Brown, S. S.; Stutz, J., Nighttime radical observations and chemistry. *Chem. Soc. Rev.*
13
14
15 602 **2012**, *41* (19), 6405-6447.
- 16
17
18 603 4. Teruel, M. A.; Lane, S. I.; Mellouki, A.; Solignac, G.; Le Bras, G., OH reaction rate
19
20
21 604 constants and UV absorption cross-sections of unsaturated esters. *Atmos. Environ.* **2006**,
22
23
24 605 *40* (20), 3764-3772.
- 25
26 606 5. Blanco, M. B.; Taccone, R. A.; Lane, S. I.; Teruel, M. A., On the OH-initiated
27
28
29 607 degradation of methacrylates in the troposphere: Gas-phase kinetics and formation of
30
31
32 608 pyruvates. *Chem. Phys. Lett.* **2006**, *429* (4-6), 389-394.
- 33
34
35 609 6. Grosjean, D.; Grosjean, E.; Williams, E. L., Rate constants for the gas-phase reaction
36
37
38 610 of ozone with unsaturated alcohols, esters, and carbonyls. *Int. J. Chem. Kinet.* **1993**, *25* (9),
39
40
41 611 783-794.
- 42
43 612 7. Gai, Y.; Ge, M.; Wang, W., Rate constants for the gas phase of ozone with n-butyl
44
45
46 613 acrylate and ethyl methacrylate. *Chem. Phys. Lett.* **2009**, *473* (1-3), 57-60.
- 47
48
49 614 8. Blanco, M. B.; Bejan, I.; Barnes, I.; Wiesen, P.; Teruel, M. A., Temperature-dependent
50
51
52 615 rate coefficients for the reactions of Cl atoms with methyl methacrylate, methyl acrylate
53
54
55 616 and butyl methacrylate at atmospheric pressure. *Atmos. Environ.* **2009**, *43* (38), 5996-6002.
- 56
57 617 9. Blanco, M. B.; Bejan, I.; Barnes, I.; Wiesen, P.; Teruel, M. A., Temperature-dependent
58
59
60

- 1
2
3
4 618 rate coefficients for the reactions of Cl atoms with methyl methacrylate, methyl acrylate
5
6
7 619 and butyl methacrylate at atmospheric pressure. *Atmos. Environ.* **2009**, *43* (38),
8
9
10 620 5996-6002.
- 11
12 621 10. Canosa-Mas, C. E.; Carr, S.; King, M. D.; Shallcross, D. E.; Thompson, K. C.; Wayne,
13
14
15 622 R. P., A kinetic study of the reactions of NO₃ with methyl vinyl ketone, methacrolein,
16
17
18 623 acrolein, methyl acrylate and methyl methacrylate. *Phys. Chem. Chem. Phys.* **1999**, *1* (18),
19
20
21 624 4195-4202.
- 22
23
24 625 11. Canosa-Mas, C. E.; Flugge, M. L.; King, M. D.; Wayne, R. P., An experimental study
25
26
27 626 of the gas-phase reaction of the NO₃ radical with alpha,beta-unsaturated carbonyl
28
29
30 627 compounds. *Phys. Chem. Chem. Phys.* **2005**, *7* (4), 643-650.
- 31
32 628 12. Wang, K.; Ge, M.; Wang, W., Kinetics of the gas-phase reactions of NO₃ radicals with
33
34
35 629 ethyl acrylate, n-butyl acrylate, methyl methacrylate and ethyl methacrylate. *Atmos.*
36
37
38 630 *Environ.* **2010**, *44* (15), 1847-1850.
- 39
40
41 631 13. Sagrario Salgado, M.; Paz Gallego-Iniesta, M.; Pilar Martin, M.; Tapia, A.; Cabanas,
42
43
44 632 B., Night-time atmospheric chemistry of methacrylates. *Environ. Sci. Pollut. Res.* **2011**, *18*
45
46
47 633 (6), 940-948.
- 48
49 634 14. Bernard, F.; Eyglunent, G.; Daele, V.; Mellouki, A., Kinetics and Products of
50
51
52 635 Gas-Phase Reactions of Ozone with Methyl Methacrylate, Methyl Acrylate, and Ethyl
53
54
55 636 Acrylate. *J. Phys. Chem. A* **2010**, *114* (32), 8376-8383.
- 56
57 637 15. Chen, H.; Ren, Y.; Cazaunau, M.; Dalele, V.; Hu, Y.; Chen, J.; Mellouki, A., Rate

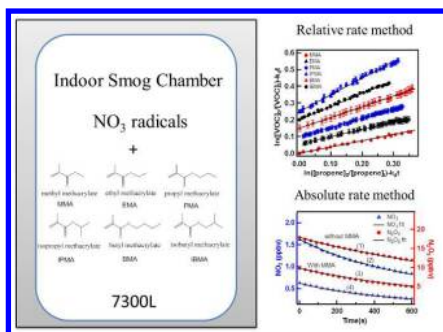
- 1
2
3
4 638 coefficients for the reaction of ozone with 2-and 3-carene. *Chem. Phys. Lett.* **2015**, *621*,
5
6
7 639 71-77.
8
9
10 640 16. Jordan, A.; Haidacher, S.; Hanel, G.; Hartungen, E.; Maerk, L.; Seehauser, H.;
11
12 641 Schottkowsky, R.; Sulzer, P.; Maerk, T. D., A high resolution and high sensitivity
13
14
15 642 proton-transfer-reaction time-of-flight mass spectrometer (PTR-ToF-MS). *Int. J. Mass*
16
17
18 643 *spectrom.* **2009**, *286* (2-3), 122-128.
19
20
21 644 17. Mueller, M.; Mikoviny, T.; Jud, W.; D'Anna, B.; Wisthaler, A., A new software tool for
22
23
24 645 the analysis of high resolution PTR-ToF mass spectra. *Chemometrics Intellig. Lab. Syst.*
25
26
27 646 **2013**, *127*, 158-165.
28
29
30 647 18. Brown, S. S.; Stark, H.; Ravishankara, A. R., Cavity ring-down spectroscopy for
31
32
33 648 atmospheric trace gas detection: application to the nitrate radical (NO₃). *Applied Physics*
34
35
36 649 *B-Lasers and Optics* **2002**, *75* (2-3), 173-182.
37
38
39 650 19. Brown, S. S.; Stark, H.; Ciciora, S. J.; McLaughlin, R. J.; Ravishankara, A. R.,
40
41
42 651 Simultaneous in situ detection of atmospheric NO₃ and N₂O₅ via cavity ring-down
43
44
45 652 spectroscopy. *Rev. Sci. Instrum.* **2002**, *73* (9), 3291-3301.
46
47
48 653 20. Brown, S. S.; Stark, H.; Ciciora, S. J.; Ravishankara, A. R., In-situ measurement of
49
50
51 654 atmospheric NO₃ and N₂O₅ via cavity ring-down spectroscopy. *Geophys. Res. Lett.* **2001**,
52
53
54 655 *28* (17), 3227-3230.
55
56
57 656 21. Brown, S. S., Absorption spectroscopy in high-finesse cavities for atmospheric studies.
58
59
60 657 *Chem. Rev.* **2003**, *103* (12), 5219-5238.

- 1
2
3
4 658 22. Fuchs, H.; Dube, W. P.; Cicioira, S. J.; Brown, S. S., Determination of inlet
5
6
7 659 transmission and conversion efficiencies for in situ measurements of the nocturnal nitrogen
8
9
10 660 oxides, NO₃, N₂O₅ and NO₂, via pulsed cavity ring-down spectroscopy. *Anal. Chem.* **2008**,
11
12
13 661 *80* (15), 6010-6017.
- 14
15 662 23. Dube, W. P.; Brown, S. S.; Osthoff, H. D.; Nunley, M. R.; Ciciora, S. J.; Paris, M. W.;
16
17
18 663 McLaughlin, R. J.; Ravishankara, A. R., Aircraft instrument for simultaneous, in situ
19
20
21 664 measurement of NO₃ and N₂O₅ via pulsed cavity ring-down spectroscopy. *Rev. Sci.*
22
23
24 665 *Instrum.* **2006**, *77* (3).
- 25
26 666 24. Fuchs, H.; Simpson, W. R.; Apodaca, R. L.; Brauers, T.; Cohen, R. C.; Crowley, J. N.;
27
28
29 667 Dorn, H. P.; Dubé, W. P.; Fry, J. L.; Häsel, R.; Kajii, Y.; Kiendler-Scharr, A. et al.,
30
31
32 668 Comparison of N₂O₅ mixing ratios during NO₃Comp 2007 in SAPHIR. *Atmos. Meas.*
33
34
35 669 *Tech.* **2012**, *5*, 2763-2777.
- 36
37 670 25. Dorn, H. P.; Apodaca, R. L.; Ball, S. M.; Brauers, T.; Brown, S. S.; Crowley, J. N.;
38
39
40 671 Dubé, W. P.; Fuchs, H.; Häsel, R.; Heitmann, U. et al., Intercomparison of NO₃ radical
41
42
43 672 detection instruments in the atmosphere simulation chamber SAPHIR. *Atmos. Meas.*
44
45
46 673 *Tech.* **2013**, *6*, 1111-1140.
- 47
48
49 674 26. Wagner, N. L.; Dube, W. P.; Washenfelder, R. A.; Young, C. J.; Pollack, I. B.; Ryerson,
50
51
52 675 T. B.; Brown, S. S., Diode laser-based cavity ring-down instrument for NO₃, N₂O₅, NO,
53
54
55 676 NO₂ and O₃ from aircraft. *Atmos. Meas. Tech.* **2011**, *4* (6), 1227-1240.
- 56
57 677 27. Davidson, J. A.; Viggiano, A. A.; Howard, C. J.; Dotan, I.; Fehsenfeld, F. C.; Albritton,
58
59
60

- 1
2
3
4 678 D. L.; Ferguson, E. E., Rate constants for reactions of O_2^+ , NO_2^+ , NO^+ , H_3O^+ , CO_3^- , NO_2^- ,
5
6
7 679 and halide ions with N_2O_5 at 300K. *J. Chem. Phys.* **1978**, *68* (5), 2085-2087.
8
9
10 680 28. Atkinson, R.; Baulch, D. L.; Cox, R. A.; Crowley, J. N.; Hampson, R. F.; Hynes, R.
11
12 681 G.; Jenkin, M. E.; Rossi, M. J.; Troe, J.; Subcommittee, I., Evaluated kinetic and
13
14
15 682 photochemical data for atmospheric chemistry: Volume II – gas phase reactions of
16
17
18 683 organic species. *Atmos. Chem. Phys.* **2006**, *6* (11), 3625-4055.
19
20
21 684 29. Burkholder, J. B.; Sander, S. P.; Abbatt, J.; Barker, J. R.; Huie, R. E.; Kolb, C. E.;
22
23
24 685 Kurylo, M. J.; Orkin, V. L.; Wilmouth, D. M.; and Wine, P. H., Chemical Kinetics and
25
26
27 686 Photochemical Data for Use in Atmospheric Studies, Evaluation No. 18," JPL Publication
28
29
30 687 15-10, Jet Propulsion Laboratory, Pasadena, **2015** <http://jpldataeval.jpl.nasa.gov>.
31
32
33 688 30. Lauraguais, A.; El Zein, A.; Coeur, C.; Obeid, E.; Cassez, A.; Rayez, M. T.; Rayez, J.
34
35
36 689 C., Kinetic Study of the Gas-Phase Reactions of Nitrate Radicals with Methoxyphenol
37
38
39 690 Compounds: Experimental and Theoretical Approaches. *J. Phys. Chem. A* **2016**, *120* (17),
40
41
42 691 2691-2699.
43
44
45 692 31. Atkinson, R., Gas-phase tropospheric chemistry of volatile organic compounds .1.
46
47
48 693 Alkanes and alkenes. *J. Phys. Chem. Ref. Data* **1997**, *26* (2), 215-290.
49
50
51 694 32. Wingenter, O. W.; Kubo, M. K.; Blake, N. J.; Smith, T. W.; Blake, D. R.; Rowland, F.
52
53
54 695 S., Hydrocarbon and halocarbon measurements as photochemical and dynamical
55
56
57 696 indicators of atmospheric hydroxyl, atomic chlorine, and vertical mixing obtained during
58
59
60 697 Lagrangian flights. *J. Geophys. Res* **1996**, *101* (D2), 4331-4340.

- 1
2
3
4 698 33. Spivakovsky, C. M.; Logan, J. A.; Montzka, S. A.; Balkanski, Y. J.; Foreman-Fowler,
5
6
7 699 M.; Jones, D. B. A.; Horowitz, L. W.; Fusco, A. C.; Brenninkmeijer, C. A. M.; Prather, M.
8
9
10 700 J.; Wofsy, S. C.; McElroy, M. B., Three-dimensional climatological distribution of
11
12 701 tropospheric OH: Update and evaluation. *J. Geophys. Res* **2000**, *105* (D7), 8931-8980.
13
14
15 702 34. Atkinson, R., Kinetics and mechanisms of the gas-phase reactions of the NO₃
16
17 703 radicals with organic compounds. *J. Phys. Chem. Ref. Data* **1991**, *20* (3), 459-507.
18
19
20 704 35. Brown, S. S.; Dubé, W. P.; Peischl, J.; Ryerson, T. B.; Atlas, E.; Warneke, C.; de Gouw,
21
22 705 J. A.; te Lintel Hekkert, S.; Brock, C. A.; Flocke, F.; Trainer, M.; Parrish, D. D.; Feshenfeld,
23
24 706 F. C.; Ravishankara, A. R., Budgets for nocturnal VOC oxidation by nitrate radicals aloft
25
26 707 during the 2006 Texas Air Quality Study. *J. Geophys. Res* **2011**, *116* (D24).
27
28
29 708 36. Martin Porrero, M. P.; Gallego-Iniesta Garcia, M. P.; Espinosa Ruiz, J. L.; Tapia Valle,
30
31 709 A.; Cabanas Galan, B.; Salgado Munoz, M. S., Gas phase reactions of unsaturated esters
32
33 710 with Cl atoms. *Environ. Sci. Pollut. Res. Int.* **2010**, *17* (3), 539-546.
34
35
36
37
38
39
40
41
42
43
44
45
46
47
48
49
50
51
52
53
54
55
56
57
58
59
60

715 TOC Graphic



716

717

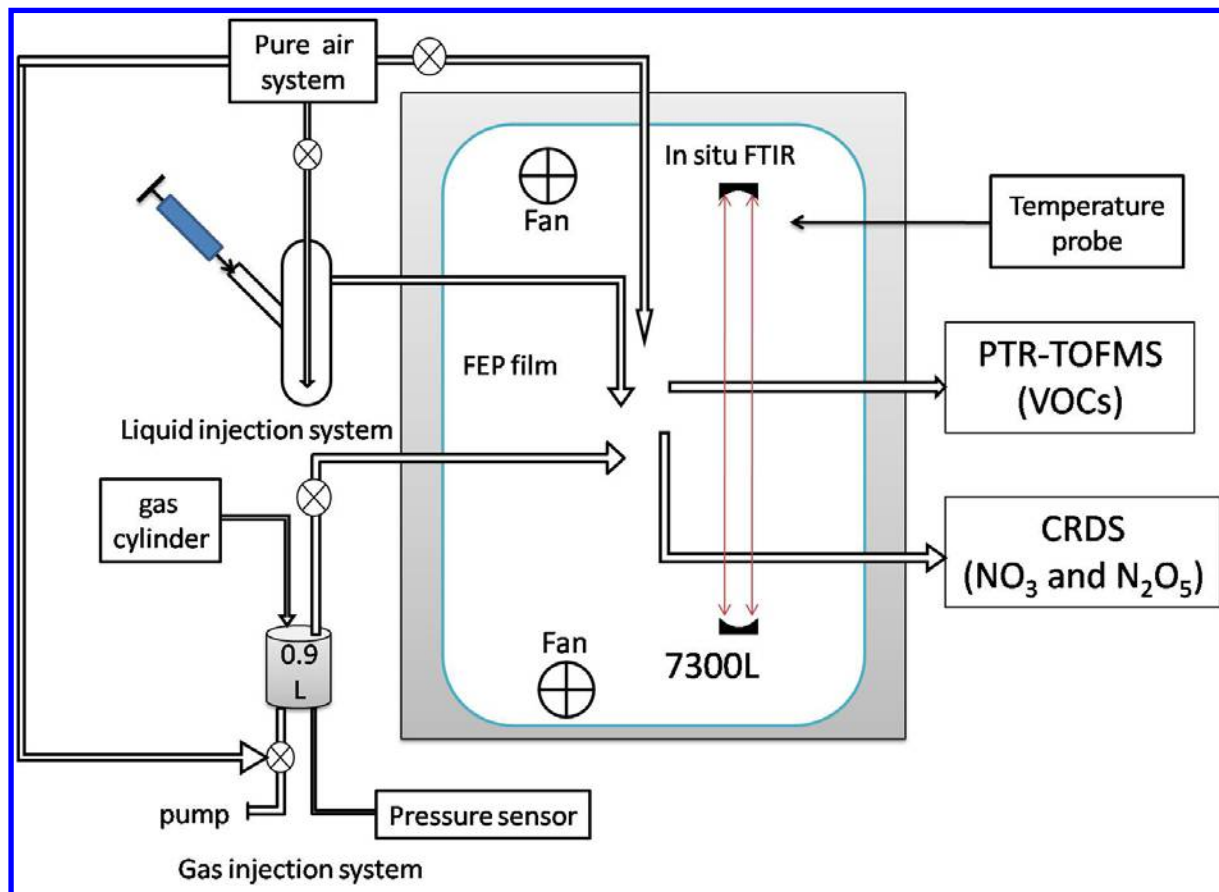
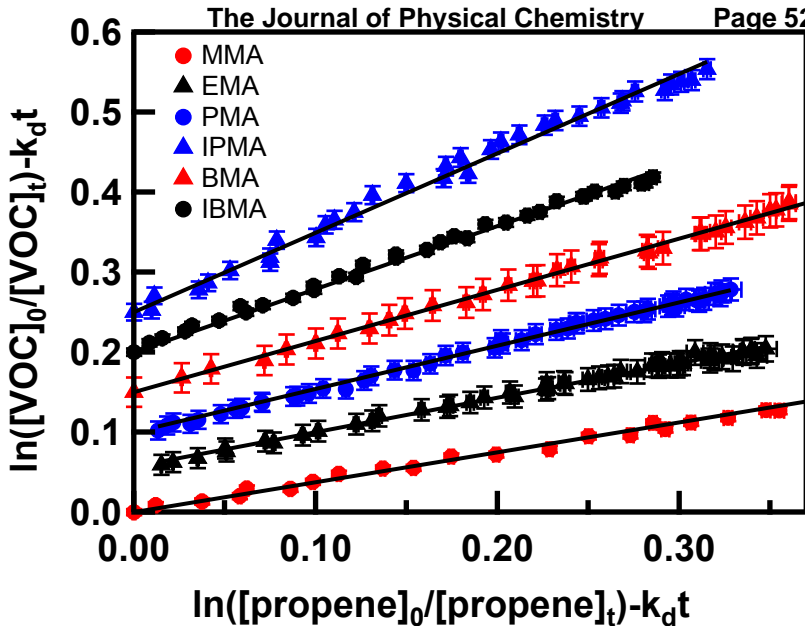
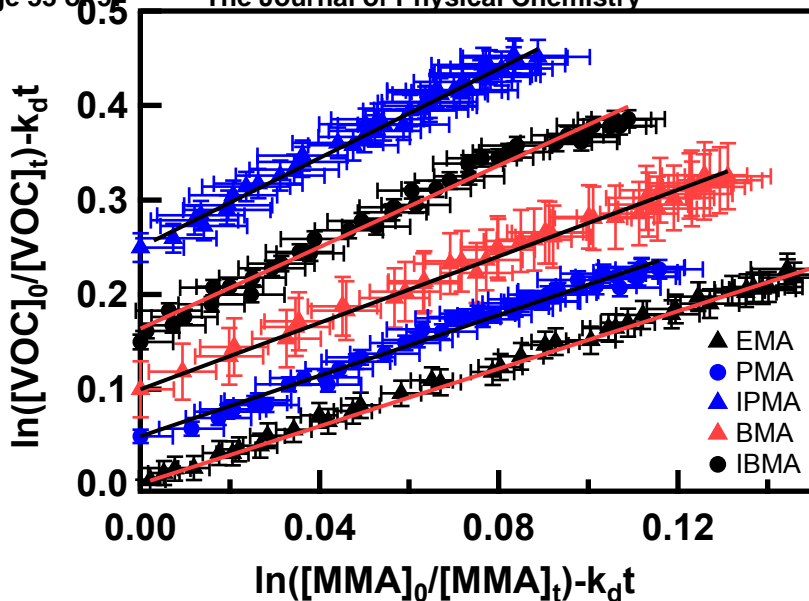


Figure 1

1
2
3
4
5
6
7
8
9
10
11
12
13
14
15
16
17
18
19
20
21
22
23
24

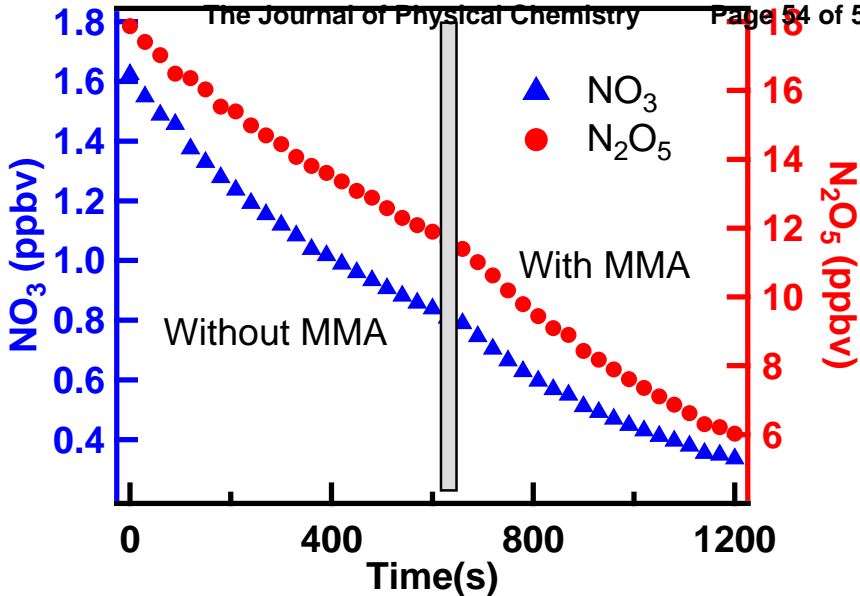
ACS Paragon Plus Environment

Figure 2-1



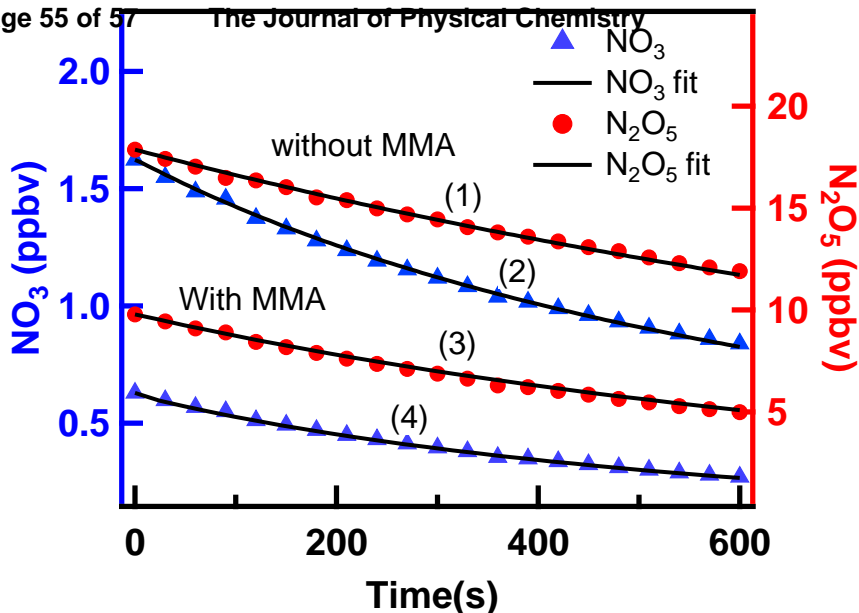
ACS Paragon Plus Environment

Figure 2-2



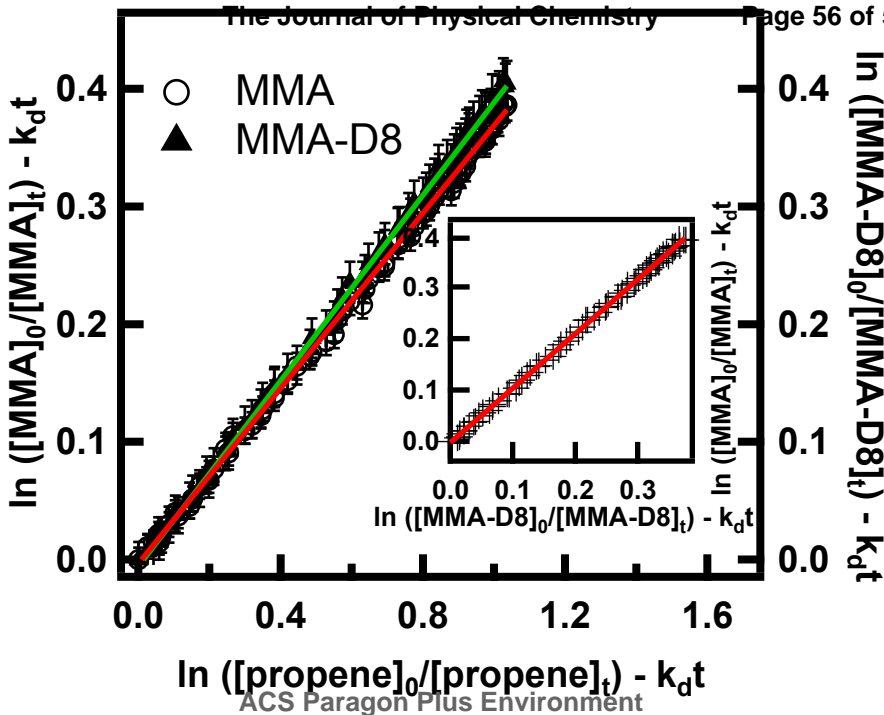
ACS Paragon Plus Environment

Figure 3



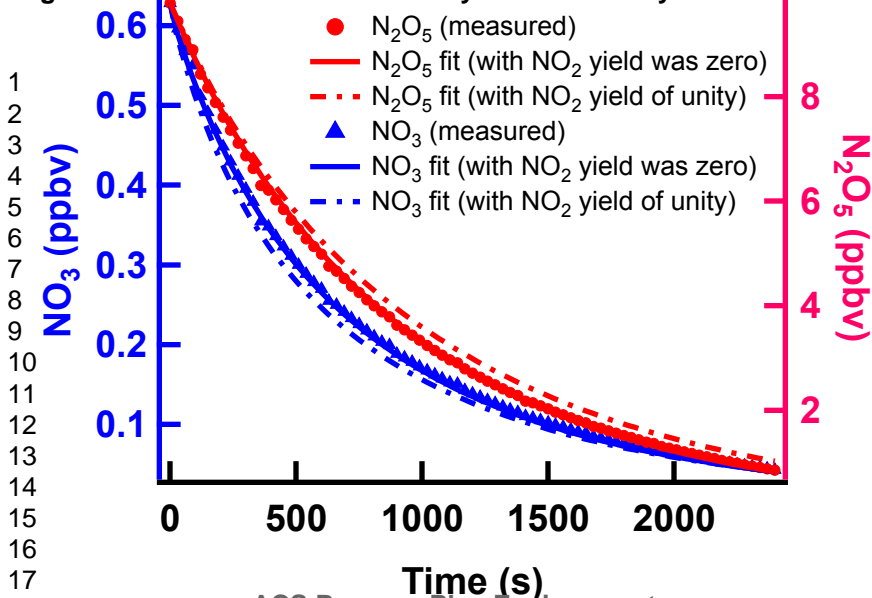
ACS Paragon Plus Environment

Figure 4

1
2
3
4
5
6
7
8
9
10
11
12
13
14
15
16
17
18
19
20
21
22
23

ACS Paragon Plus Environment

Figure 5



ACS Paragon Plus Environment

Figure 6